β-decay studies of neutron-rich Tl, Pb, and Bi isotopes

A. I. Morales,[1,2,*] G. Benzoni,[1] A. Gottardo,[3,4] J. J. Valiente-Dobón,[3] N. Blasi,[1] A. Bracco,[1,2] F. Camera,[1,2] F. C. L. Crespi,[1,2] A. Corsi,[1,2] S. Leoni,[1,2] B. Million,[1] R. Nicolini,[1,2] O. Wieland,[1] A. Gadea,[5] S. Lunardi,[4,6] M. Górska,[7] P. H. Regan,[8,9] Zs. Podolyák,[8] M. Pfützner,[10] S. Pietri,[7] P. Boutachkov,[7] H. Weick,[7] J. Grebosz,[11] A. M. Bruce,[12] J. Alcántara Núñez,[13] A. Algora,[5,14] N. Al-Dahan,[8] Y. Ayyad,[13] N. Alkhomashi,[8,15] P. R. P. Allegro,[16] D. Bazzacco,[6] J. Benlliure,[13] M. Bowry,[8] M. Bunce,[8] E. Casarejos,[17] M. L. Cortes,[7] A. M. Denis Bacelar,[12] A. Y. Deo,[8,†] G. de Angelis,[3] C. Domingo-Pardo,[7] M. Doncel,[18] Zs. Dombradi,[19] T. Engert,[7] K. Eppinger,[20] G. F. Farrelly,[8] F. Farinon,[7] E. Farnea,[6] H. Geissel,[7] J. Gerl,[7] N. Goel,[7] E. Gregor,[7] T. Habermann,[7] R. Hoischen,[7,21] R. Janik,[22] S. Klupp,[23] I. Kojouharov,[7] N. Kurz,[7] S. Mandal,[24] R. Menegazzo,[6] D. Mengoni,[6] D. R. Napoli,[3] F. Naqvi,[7,25] C. Nociforo,[7] A. Prochazka,[7] W. Prokopowicz,[7] F. Recchia,[6] R. V. Ribas,[16] M. W. Reed,[8] D. Rudolph,[21] E. Sahin,[3] H. Schaffner,[7] A. Sharma,[7] B. Sitar,[22] D. Siwal,[24] K. Steiger,[20] P. Strmen,[22] T. P. D. Swan,[8] I. Szarka,[22] C. A. Ur,[6] P. M. Walker,[8] and H.-J. Wollersheim[7]

[1]*Istituto Nazionale di Fisica Nucleare, Sezione di Milano, Milano, Italy*
[2]*Dipartimento di Fisica dell'Università degli Studi di Milano, Milano, Italy*
[3]*Istituto Nazionale di Fisica Nucleare, Laboratori Nazionali di Legnaro, Legnaro, Italy*
[4]*Dipartimento di Fisica dell'Università degli Studi di Padova, Padova, Italy*
[5]*Instituto de Física Corpuscular, CSIC-Universitat de València, València, Spain*
[6]*Istituto Nazionale di Fisica Nucleare, Sezione di Padova, Padova, Italy*
[7]*GSI Helmholtzzentrum für Schwerionenforschung, Darmstadt, Germany*
[8]*Department of Physics, University of Surrey, Guildford, United Kingdom*
[9]*National Physical Laboratory, Teddington, United Kingdom*
[10]*Faculty of Physics, University of Warsaw, Warsaw, Poland*
[11]*Niewodniczanski Institute of Nuclear Physics, Polish Academy of Science, Krakow, Poland*
[12]*School of Computing, Engineering, and Mathematics, University of Brighton, Brighton, United Kingdom*
[13]*Universidad de Santiago de Compostela, Santiago de Compostela, Spain*
[14]*Institute of Nuclear Research of the Hungarian Academy of Sciences, Debrecen, Hungary*
[15]*KACST, Riyadh, Saudi Arabia*
[16]*Instituto de Fisica, Universidade de São Paulo, São Paulo, Brazil*
[17]*EEI, Universidade de Vigo, Vigo, E-36310, Spain*
[18]*Laboratorio de Radiaciones Ionizantes, Universidad de Salamanca, Spain*
[19]*Institute for Nuclear Research, Hungarian Academy of Sciences, Debrecen, Hungary*
[20]*Physik Department, Technische Universität München, Garching, Germany*
[21]*Department of Physics, Lund University, Lund, Sweden*
[22]*Faculty of Mathematics and Physics, Comenius University, Bratislava, Slovakia*
[23]*Physik-Department E12, Technische Universität München, Garching, Germany*
[24]*Department of Physics and Astrophysics, University of Delhi, Delhi, India*
[25]*Institut für Kernphysik, Universität zu Köln, Köln, Germany*

(Received 23 September 2013; revised manuscript received 19 December 2013; published 29 January 2014)

The fragmentation of relativistic uranium projectiles has been exploited at the Gesellschaft für Schwerionenforschung laboratory to investigate the β decay of neutron-rich nuclei just beyond ^{208}Pb. This paper reports on β-delayed γ decays of $^{211–213}$Tl, ^{215}Pb, and $^{215–219}$Bi de-exciting states in the daughters $^{211–213}$Pb, ^{215}Bi, and $^{215–219}$Po. The resulting partial level schemes, proposed with the help of systematics and shell-model calculations, are presented. The role of allowed Gamow-Teller and first-forbidden β transitions in this mass region is discussed.

DOI: 10.1103/PhysRevC.89.014324 PACS number(s): 27.80.+w, 23.40.−s, 23.20.Lv, 26.30.Hj

I. INTRODUCTION

The nuclear region beyond doubly magic ^{208}Pb represents a fertile testing ground in nuclear physics to trace the evolution of the 82-proton shell closure on the way to reflection asymmetric configurations [1,2]. While the structure of ^{208}Pb is well understood in terms of the spherical shell model, experimental data on heavier nuclei are very scarce. It is still an open question to what extent shell model calculations hold as the complexity of the valence space increases. On top of that, the β decay in this region attracts great attention for astrophysical purposes: It is well established that the *r*-process path lies very far from accessible nuclei. Therefore, theoretical models have to extrapolate extensively in order to provide nuclear inputs for *r*-process calculations. Predictions of time scales and production rates can vary over orders of magnitude depending on the nuclear framework employed. Whereas standard microscopic-macroscopic models emphasize the importance of the allowed Gamow-Teller β-decay strength [3],

*anaisabel.morales@mi.infn.it
†Present address: Department of Physics, Indian Institute of Technology Roorkee, Roorkee 247 667, India.

self-consistent microscopic treatments stress the role of first-forbidden transitions in the reduction of predicted lifetimes [4,5]. From an experimental viewpoint, this issue is also a source of debate: Recent β-decay studies for $N < 126$ nuclei hint at a substantial contribution of forbidden transitions to the total β strength [6,7], while half-life measurements beyond ^{208}Pb [8–10] point towards a more complex landscape where the interplay between allowed and first-forbidden decays depends on the differing valence configurations. Detailed information on β-decay strength functions and Q_β values is required in order to address the present discrepancies between theory and experiment.

The first structural information on the neutron-rich Pb-Po isotopes came from natural radioactive decay chains. More recent attempts to populate this region have exploited deep-inelastic reactions induced on both ^{208}Pb and ^{238}U targets [11], yet the charge equilibration process is known to drive the reaction products towards stability. While the relatively long expected lifetimes would make these nuclei adequate candidates to be produced with the isotope separation on-line method, the so-called ISOL technique, few successful experiments have been performed so far [9,10,12–14]. These studies employed Pb and Bi radioactive beams for β-decay spectroscopy, using the pulsed release technique to minimize the isobaric contamination. Cold fragmentation reactions have been used as well to synthesize $N > 126$ nuclei [15,16]. The cited experiments, however, could give structural information only up to ^{212}Pb, owing to technical difficulties, such as low primary beam intensity and low detection efficiency.

The present work aims at extending the scarce spectroscopy data beyond ^{208}Pb by exploiting the in-flight fragmentation of a relativistic ^{238}U beam delivered by the SIS18 syncrotron at the Gesellschaft für Schwerionenforschung (GSI). This experimental approach has proven to be an alternative, very efficient tool to synthesize and study heavy exotic neutron-rich species. Results on the β decays $^{211–213}$Tl $\rightarrow$ $^{211–213}$Pb, ^{215}Pb $\rightarrow$ ^{215}Bi, and $^{215–219}$Bi $\rightarrow$ $^{215–219}$Po are presented and discussed here. Earlier investigations on some of the cited nuclei exploited deep-inelastic [17] and transfer [18,19] reactions, α decay [2,20–24], and β decay [9,10,12–14,25]. In particular, this work reports on the first spectroscopic information on ^{213}Pb and ^{219}Po. Note that even if not extremely neutron-rich, being just few neutrons away from the stability line, these are the most exotic nuclei so far accessible for spectroscopy studies.

This wealthy dataset has already provided some important results, such as the identification of seniority isomers along the neutron-rich Pb chain [26], the measurement of β half-lives in neutron-rich Tl and Bi isotopes [8], and the observation of new μs isomers in the neutron-rich ^{210}Hg nucleus [27].

The current paper is organized as follows: In Sec. II a brief description of the experimental conditions and set up is given. Section III focuses on the description of the data analysis. A dedicated paragraph on the β-decay half-life of ^{215}Pb, obtained from ion-α correlations, is presented in Sec. IV. In Sec. V the β-decay spectroscopic results are shown. Section VI is devoted to the discussion of proposed level schemes, and Sec. VII gives the final remarks and conclusions.

II. EXPERIMENTAL DETAILS

The experiment here described exploited a fragmentation reaction of a ^{238}U beam at 1 GeV/nucleon on a 2.5 g/cm^2 Be target. The ^{238}U beam was delivered by the UNILAC-SIS accelerators at a stable intensity of 1.5×10^9 ions/spill, with a repetition cycle of 3 s and an extraction time of 1 s.

The nuclei of interest were separated and identified in the magnetic spectrometer fragment separator (FRS) [28]. The FRS consists of two double-dipole stages with a variable-thickness and variable-profile degrader between. The FRS separates the nuclei by means of the $B\rho$-ΔE-$B\rho$ scheme and can be operated both in achromatic and monochromatic modes.

A 758 mg/cm^2 Al wedge-shaped degrader was set at the intermediate focal plane to produce a monochromatic beam, ensuring the simultaneous implantation of the species in an active stopper located at the final focal plane of the FRS. This degrader was used to resolve the different atomic charge-state configurations that hinder the identification of heavy species, using the procedure detailed in Ref. [29]. An additional homogeneous 2.4 g/cm^2 Al degrader was placed after the first dipole of the FRS in order to reduce the count rate in the intermediate focal plane detectors, arising mainly from primary-beam charge states (^{238}U^{91+} and ^{238}U^{90+}).

The standard FRS equipment, comprising in the intermediate and final focal planes thin scintillator detectors for time-of-flight measurement, time projection chambers for position determination, and ionization chambers for energy-loss measurements, was employed.

The nuclei of interest were transported to the final focal plane where the stopped-beam RISING (rare isotope investigations at GSI) setup [30] was placed. The fragmentation residues were slowed down in a variable-thickness Al degrader to the energies required to implant the selected nuclei in the RISING active stopper [31], a composite system of nine double-sided silicon strip detectors (DSSSD), all of dimensions 5×5 cm^2 and 1 mm thickness. These detectors were arranged in three rows of three elements each. Each DSSSD consisted of 16 front strips and 16 back strips, each with a width of 3 mm, thus providing 256 pixels to encode the x and y position information. The Si detectors were used to identify both implantations and β-decay events. Moreover, the array was employed to measure the α particles emitted by the decay-chain daughters of the fragmentation residues. This poses stringent requirements on the electronics since the device has to deal with signals generated by either electrons or α particles of few MeV energy, and nuclei of energies in the GeV range. MESYTEC MPR-32 logarithmic preamplifiers, which are linear up to 10 MeV and then have a logarithmic response in the implantation regime, were employed [31]. While they are not suited to measure the total energy loss, they allow one to disentangle the three different signals released by implantations, α particles, and β electrons without saturating the modules. Two scintillation detectors were placed in front of and behind the DSSSD array (this last is referred to as "veto scintillator" later in the text) to reject unwanted reaction products induced by the implantation process.

The RISING γ array, composed by 105 HPGe detectors grouped in clusters of seven elements each, surrounded the

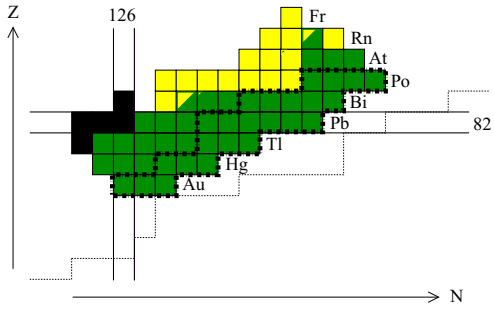

FIG. 1. (Color online) Nuclear region investigated in the present experiment. Residues formed in the fragmentation reaction are delimited by a thick dot-dashed line, whereas decay successors lie outside. Green (gray) and yellow (light gray) boxes stand for β and α emitters, respectively. Stable nuclei are marked by black squares. The black dashed line shows the limit of nuclei so far synthesized.

active stopper. The full-energy peak detection efficiency of the spectrometer was measured to be 15% at 662 keV [30]. This array enabled the measurement of γ-ray transitions in time coincidence with implantations or radioactive particles, during a correlation time window of up to 100 μs. More details on the experimental setup can be found in Refs. [7,8,26,30,32].

A number of isotopes for each nuclear species, ranging from Au ($Z = 79$) to Po ($Z = 84$), were populated and implanted for subsequent β-decay spectroscopy. Their location in the nuclear chart is shown in Fig. 1 by a dot-dashed line.

III. CORRELATION PROCEDURE

As shown in Fig. 1, the unstable Tl-Pb-Bi isotopes undergo several β and α decays, producing new radioactive species until a stable or long-lived nucleus is formed. The identification of the implanted fragments, the emitted particles, and the coincident γ rays was exploited to define different types of time and position correlations. These allowed for the extraction of half-lives and β-delayed γ transitions, employing the delayed-coincidence technique.

As in other β-decay studies with the RISING setup [7,8,32,33], implantations were accepted when one pixel of the DSSSD detectors registered a high-energy event in coincidence with a signal under particle threshold in the veto scintillator. The electrons emitted in their decay deposit typically several hundreds of keV in the active stopper. Based on this, matching β electrons were defined as events with an energy signal below 2 MeV recorded in the pixel activated by the implantation or in the eight neighboring cells. The α decays, instead, were accepted when a discrete energy signal in the 5- to 10-MeV range was recorded in the implantation pixel. An event-by-event basis was used to record the information on the energy, position, and time of all types of events. The correlation time for β-delayed γ-ray spectroscopy was chosen according to the known half-lives, being usually $T_{\rm corr} = 3T_{1/2}$. The ion-β correlations were employed to study the decay of the fragmentation residues $^{211–213}$Tl, ^{215}Pb, and ^{218,219}Bi. Such nuclei are characterized by long β-decay half-lives [8] that induce correlation intervals up to several hundred times longer than the beam cycle, thus increasing the number of δ or

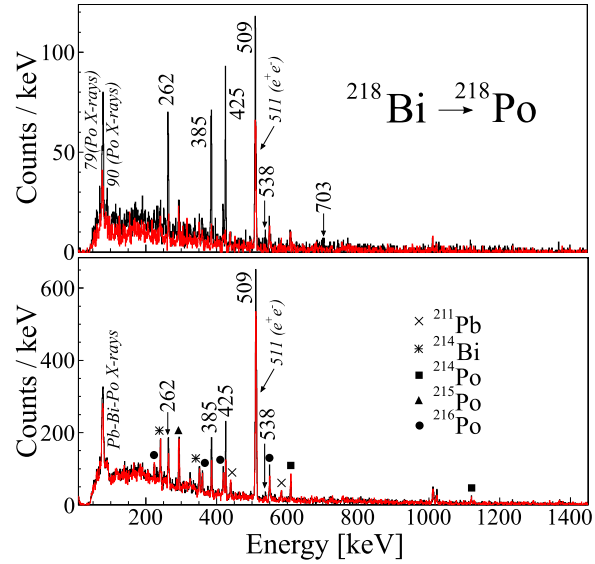

FIG. 2. (Color online) β-delayed γ spectra following the decay ^{218}Bi$\rightarrow^{218}$Po. Black spectra include ion-β correlations sorted in correct time order, while red (gray) spectra are sorted in reverse time mode to account for the background. The upper panel includes only ion-β correlations within the implantation pixels, while the lower panel also incorporates contributions from the eight adjacent cells. The energies of the transitions belonging to this specific decay are indicated, while contaminant peaks are labeled by symbols.

accidental β electrons in the spectra. To resolve the specific γ transitions from the random contribution of other radioactive species, the β-like events recorded during the beam-on periods were excluded from the data analysis. Second, even if an average of 60% matching β particles were registered in the neighbor pixels, the position correlations were limited to the implantation cell. The remaining background could be evaluated by sorting the data in reverse-time sequence [7,8]. The reverse-time background technique consists in correlating the implantation events with valid β candidates registered previously in the active stopper. Since the experimental conditions are equal, the γ spectra sorted in reverse-time mode represent the random background of the γ spectra in the normal time direction.

The effect of these correlation conditions is illustrated in Fig. 2, which compares the β-delayed γ spectra of ^{218}Bi obtained with and without the β particles detected on the adjacent pixels. The spectra obtained by sorting the data in the normal time sequence are shown with a black line, while reversed-time background is shown with a red (gray) line. In both panels specific transitions attributed to ^{218}Po [9] are visible. In the upper panel, that includes only β-γ coincidences where the electron was detected in the implantation pixel, the transitions associated with the decays of the selected nucleus are well resolved from the β-like background, while in the bottom panel, which incorporates the contribution of events where the β electron was detected in a pixel neighboring the implantation one, many γ lines from other nuclei appear.

The direct access to β-decay information in some of the nuclei of interest was hindered because of either very

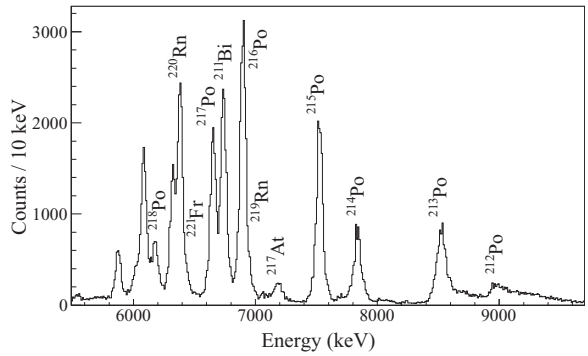

FIG. 3. Energy spectrum of the active stopper zoomed in on the energy region of α decay. Labelled peaks correspond to known α lines. The nuclei ^{212,213}Po, with α decay lifetimes shorter than the time gate of the digital γ finder modules (100 μs), show a continuous tail extending to higher energies, corresponding to the pileup of β and α particles.

long lifetimes or high β background arising from the high implantation rates of neighboring nuclei. For these cases, namely $^{215-217}$Po, ion-β correlations were not sufficient and an additional tag to the emitted α particles was required.

A typical α-particle energy spectrum measured in the active stopper is shown in Fig. 3. In contrast to the β-tagging procedure described in Refs. [7,8], the clear identification of the α particles in position and energy reduces significantly the background contribution from other nuclear species. Since the range of an α particle in silicon is only of 30–60 μm, the α correlations can be restricted to the pixel of implantation while maintaining a detection efficiency close to 100%. The only background contributions to be considered are due to the presence of other fragments decaying to the same α emitter. For instance, Fig. 4 illustrates the decay patterns of the fragmentation residues leading to ^{216}Po. These are ^{216}Pb, ^{216}Bi, and ^{220}Po. The random correlations originating from this background form an exponential time distribution function with a decay constant mainly given by the frequency of implantation of the contaminant species, which is typically 1×10^{-4} s^{-1} to 5×10^{-4} s^{-1}. Further details are given in Ref. [34].

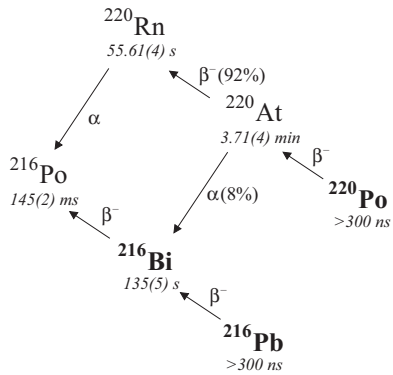

FIG. 4. The decay series to ^{216}Po. Nuclei in bold are fragmentation residues implanted in the active stopper.

IV. β-DECAY HALF-LIFE OF ^{215}Pb

The nucleus ^{215}Pb was recently studied at CERN [10], exploiting spallation of relativistic protons on a thick UC_x target. The combination of the resonant ionization laser ion source and the pulsed release method reduced the isobaric contamination of ^{215}Pb to a level sufficiently low for β-decay spectroscopy. Its half-life, $t_{1/2} = 147(12)$ s, and the apparent β feedings and log ft values of the low-spin states populated in the daughter ^{215}Bi, were measured.

The case of ^{215}Pb is particularly appealing to benchmark the α-tagging technique since typical ion-β-γ correlations do not provide a reasonable half-life measurement given the long correlation times involved and the high β feeding of the ^{215}Bi ground state [10]. Further correlations to the successive α particles of ^{215}Po are thus necessary.

The α decay of ^{215}Po is characterized by the emission of an α particle of 7526.3(8) keV that feeds the ground state of ^{211}Pb with a half-life of 1.781(4) ms [35]. Because of the prompt nature of the process, the β-α correlations can be extended to a greater range of beam spills and neighboring cells without extra cost in contaminant activity. Indeed, only 0.14% of the accepted β electrons have multiplicity $m \geqslant 2$ within the correlation time gate.

The α-tagged β electrons, corresponding to the decay of ^{215}Bi, are then correlated with the first implantation of ^{215}Pb registered in the pixel hit by the α particle. In this way, the time behavior of the ion-β correlations can be expressed in terms of the decay constants of ^{215}Pb and ^{215}Bi through the Bateman equations [36]. Note that the half-life of ^{215}Bi^{gs} was previously reported as 456(12) s [25], so the only unknown fitting parameter is the lifetime of ^{215}Pb. The background arising from the random contributions of other α precursors, namely ^{215}Bi, ^{219}Bi, and ^{219}Po, is accounted for by adding an exponential time distribution function, as explained in the previous section.

Figure 5 shows the activity of the daughter ^{215}Bi relative to the implantation of ^{215}Pb fragments. The fit is shown as a continuous line. For the sake of clarity, the background is indicated as a dashed line. The half-life of ^{215}Pb extracted from the least squares fit is $t_{1/2} = 160(40)$ s. The uncertainty is obtained from both statistical errors related to the analytical

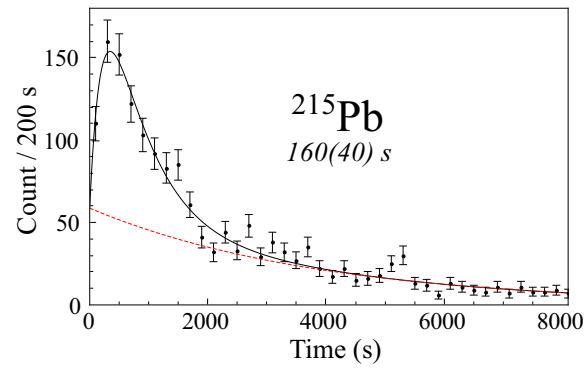

FIG. 5. (Color online) Time distribution of ^{215}Pb relative to the activity of the 7.6-min β daughter ^{215}Bi. See text for details on the least squares fit.

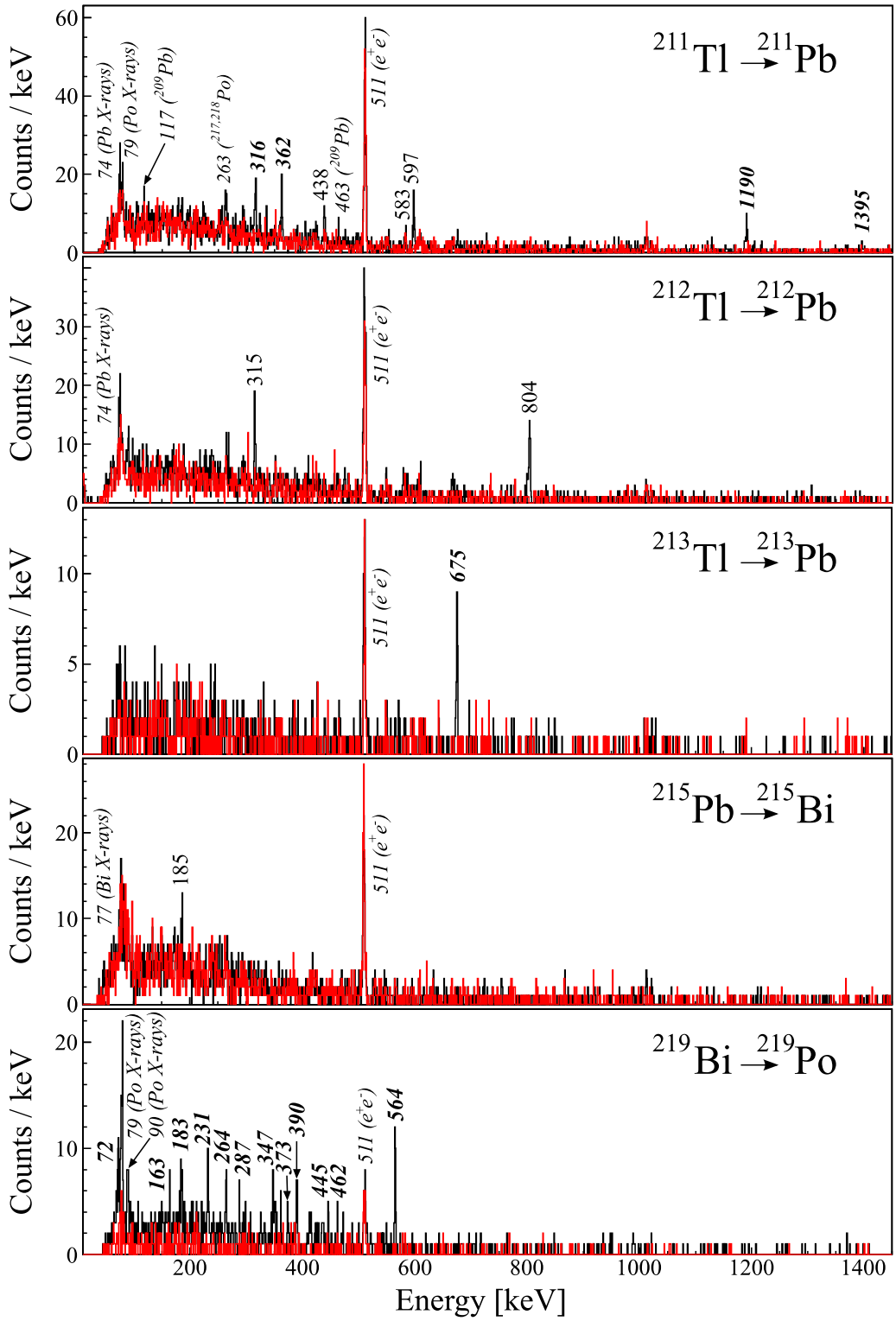

FIG. 6. (Color online) β-delayed γ spectra of $^{211–213}$Tl, ^{215}Pb, and ^{219}Bi showing γ decays in the daughter nuclei $^{211–213}$Pb, ^{215}Bi, and ^{219}Po. The γ peaks labeled in normal font were observed in former studies, whereas those shown in bold are reported for the first time in this work. X rays and contaminant peaks are indicated in italics. The reversed-time background is shown with the red (gray) line.

fit and systematic errors arising from the finite bin size. Note that this value confirms the recently reported half-life of $t_{1/2} = 147(12)$ s [10] using an independent method of production and data analysis.

V. β-DELAYED γ SPECTRA

Here we report the β-delayed γ-ray energy spectra collected from either ion-β or β-α correlations. These results

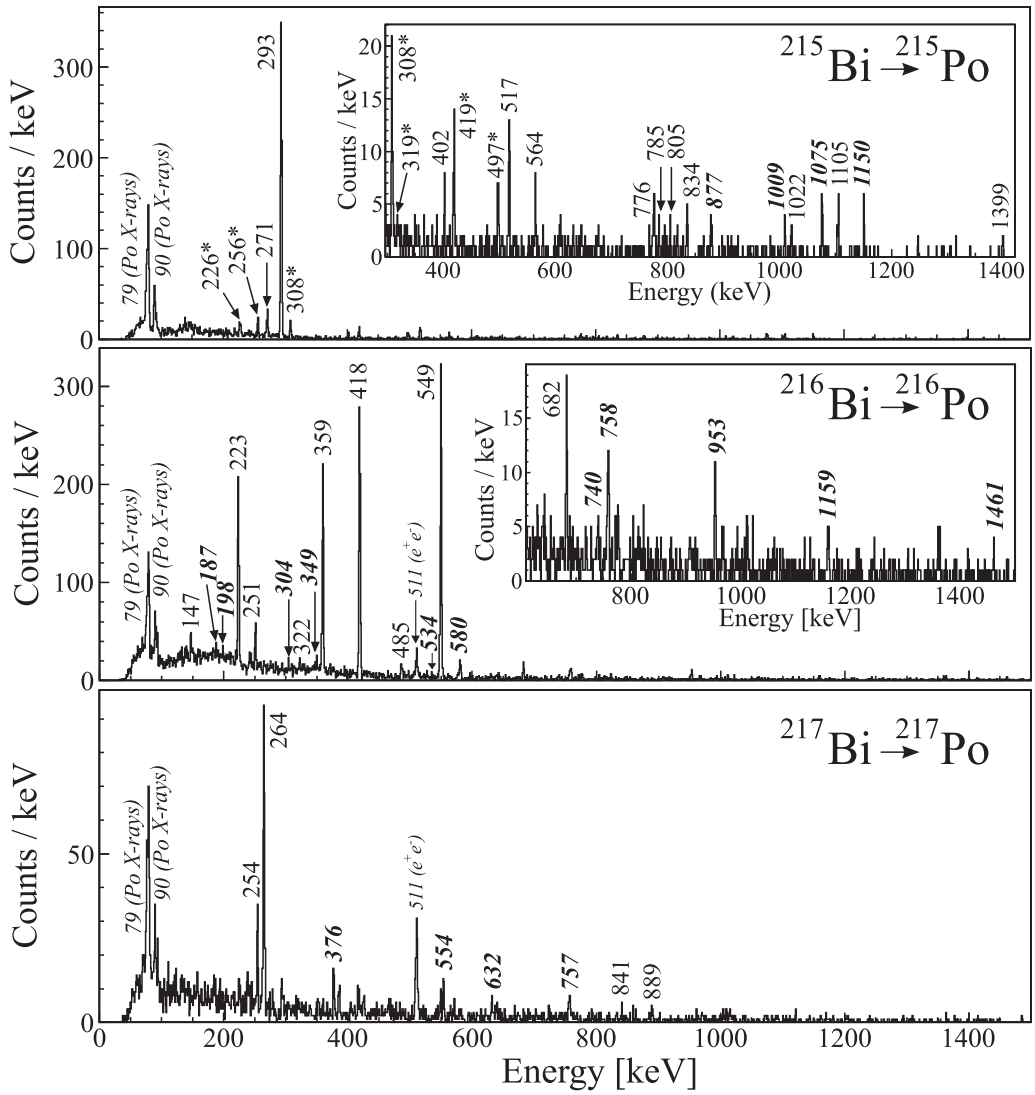

FIG. 7. β-delayed γ spectra of $^{215-217}$Bi showing γ decays in the daughters $^{215-217}$Po. For these nuclei, an additional tag to the α particles emitted by the Po successors is applied. The γ peaks labeled in normal font were observed in former studies, whereas those shown in bold are reported for the first time in this work. X rays and contaminant peaks are indicated in italics. Transitions marked with an asterisk in the upper panel are interpreted as de-exciting a state populated from a β-decaying high spin isomer in ^{215}Bi [13].

bring to completion the β decay studies on the fragmentation residues $^{211-213}$Tl and $^{215-219}$Po, for which the half-lives are reported elsewhere [8,34].

The β-delayed γ spectra of $^{211-213}$Tl $\rightarrow$ $^{211-213}$Pb, ^{215}Pb $\rightarrow$ ^{215}Bi, and ^{219}Bi $\rightarrow$ ^{219}Po are shown in Fig. 6. The black spectra show ion-β correlated γ rays sorted in normal time order, while the red (gray) spectra are built from reverse-time correlations to indicate the random background. The β-delayed γ spectra of $^{215-217}$Bi, showing γ-ray transitions in the decay daughters $^{215-217}$Po, are shown in Fig. 7. At variance with the nuclei cited above, the spectra are obtained from β-α correlations. The short lifetimes of the $^{215-217}$Po α emitters [35] allow for an unequivocal tag of the β particles previously emitted by the Bi progenitors. Further β-γ correlations enable the identification of specific γ rays in $^{215-217}$Po.

Starting from the top panel of Fig. 6, three transitions were observed following α decay of ^{215}Po [20]: The $(7/2)^+ \rightarrow 9/2^+$ at 438 keV, one at 583 keV, and the $(5/2^+) \rightarrow 9/2^+$ at 597 keV in ^{211}Pb. The γ peaks at 315 and 804 keV in ^{212}Pb were recently identified as the $(4^+) \rightarrow (2^+) \rightarrow 0^+$ members of the γ cascade de-exciting a 8^+ seniority isomer [26]. The 185-keV $(7/2^-) \rightarrow (9/2^-)$ ground-state transition in ^{215}Bi confirms the observations of recent β-decay studies [10].

For the Po isotopes (shown in Figs. 2 and 7), former β-decay works provide extensive information on excited states and γ rays [9,12–14,25]. In the case of ^{215}Po, the transitions labeled with an asterisk were reported before in the β decay of the 36.9 s high-spin isomer $J^\pi = (25/2^-, \ldots, 29/2^-)$ of ^{215}Bi [13]. Here, they confirm its population in relativistic fragmentation of uranium. In our study, however, only one of the two states populated in ^{215}Po is observed, at 1999 keV (in Ref. [13] it is reported at 2001.2 keV). No hint of the population of the 2159.4-keV level has been found, since the 158.2-keV transition de-exciting this state is not observed. The subsequent

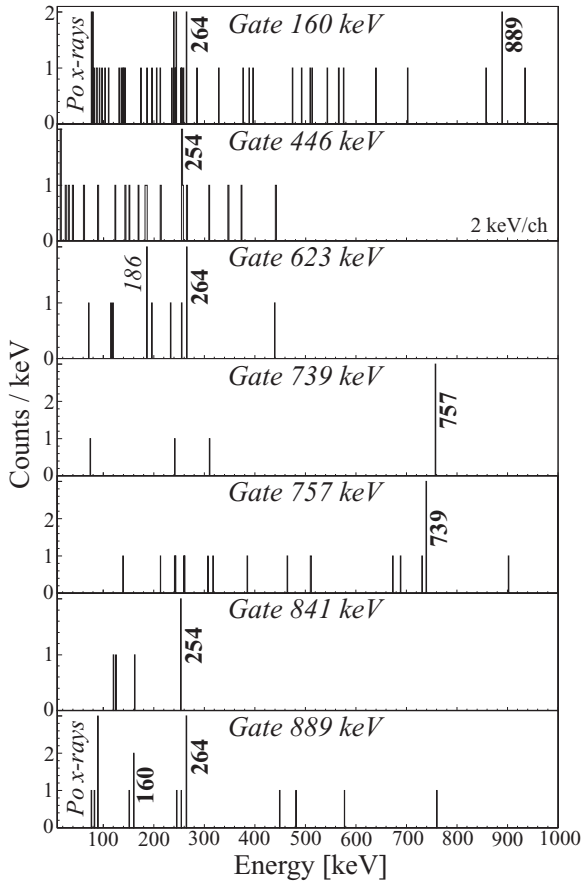

FIG. 8. The γ-ray spectra in coincidence with the 160-, 446-, 623-, 739-, 757-, 841-, and 889-keV transitions tentatively attributed to ^{217}Po. Only γ rays followed by an α particle of ^{217}Po are included. X rays are labeled in italics.

319.1 → 178.7 keV cascade feeding the $(23/2^-)$ level is not seen. This can be understood in terms of the absolute intensities reported in the previous work: The intensity of the 308-keV γ peak is five times larger than the intensity of the 319-keV transition. As this γ line does not emerge from the observed background, one does not expect to resolve the other peaks with similar intensities and lower energies either. From the ratio between the intensities of the 226- and 293-keV γ lines one can infer an isomeric ratio of 36–43(3)% for the production of the high-spin isomer of ^{215}Bi. Since the spectrum shown in Fig. 7 includes the contributions from all the ^{215}Po precursors, the intensity of the 293-keV transition has been normalized to the accumulated statistics for the ^{215}Bi residues. The lower limit, then, is given by an extreme situation in which all the 293-keV γ intensity comes from the de-excitation of the high-spin isomer, while the upper limit corresponds to the opposite case, in which all the intensity arises from the decay of the ^{215}Bi ground state. It is worth noting the agreement between the values obtained from the β-delayed γ spectra shown here and from the time decay curve of ^{215}Bi, discussed in Ref. [34].

The analysis of γ-γ coincidences has allowed some γ-decay relationships between new and previously reported transitions to be established. As an illustration, Fig. 8 shows the α-tagged γ spectra in coincidence with the 160-, 446-, 623-, 739-, 757-, 841-, and 889-keV γ peaks in ^{217}Po, using a coincidence time interval of 100 ns. Note that the transitions at 160, 446, 623, and 739 keV are not clearly visible above background in Fig. 7. However, they are included in the level scheme of ^{217}Po based on their coincidence relationships. The same situation arises for the 157-keV γ ray in ^{212}Pb, the 785- and 805-keV transitions in ^{215}Po, and the 428- and 740-keV γ rays in ^{216}Po.

Tables I and II list the energies, relative intensities (where possible), and coincidence relationships of the γ transitions observed in this work. Relative intensities of the transitions marked with an asterisk were obtained from γ-γ coincidences, while transitions which do not show firm coincidence relations are shown with a dagger.

VI. LEVEL SCHEMES AND DISCUSSION

Tentative level schemes for $^{211–213}$Pb and $^{215–218}$Po have been deduced from the information summarized in Tables I and II. They are presented in Figs. 9, 10, and 11. Spins and parities have been proposed with the help of systematics, shell-model calculations, and/or the angular momentum transfers allowed by the β interaction, which are typically 0 or 1 units in the region of interest [37]. If possible, tentative γ-ray multipolarities and apparent β feedings, estimated from transition intensity balances, are provided. Note that level orderings differing from those presented here cannot be definitely excluded.

For $^{211–213}$Pb, shell-model calculations using the code ANTOINE [38] are compared to the experimental levels. The modified Kuo-Herling effective interactions [39], which were successfully used to describe some moderately neutron-rich nuclei beyond lead, are employed in a model space consisting of the full major-shell above $N = 126$ upon the doubly magic ^{208}Pb inert core. The single-particle energies of the valence orbitals are taken from the excitation energy spectrum of ^{209}Pb [39].

Shell-model calculations for the Po isotopes were at the limits of computational operation due to the large number of valence nucleons beyond the $Z = 82$ and $N = 126$ closed shells. Furthermore, α-decay studies have proven that these nuclei are already on the lower-left edge of the island of reflection asymmetry, presenting a dominant shell-model character with residual components of reflection-asymmetric configurations [2]. Their structure, thus, is discussed only in terms of already reported spectroscopic information and systematics.

A. Decays $^{211–213}$Tl → $^{211–213}$Pb

Four new transitions at 316, 362, 1190, and 1395 keV have been observed following the β decay of ^{211}Tl. Their placement in the level scheme of Fig. 9 is based on coincidence relations with the previously reported γ rays, as well as on relative intensities. They provide evidence for the population of three new excited states at 754, 1787, and 2149 keV, as summarized in Table I.

From systematics and shell-model predictions, the mother ^{211}Tl is expected to have a $1/2^+$ ground state. Shell model

TABLE I. Level energies E_x, γ-ray energies E_γ, relative γ intensities (normalized to the most intense γ peak) I_γ, and coincidence relations of the γ rays observed in this work. An asterisk (*) marks intensities deduced from γ-γ coincidences. A dagger (†) indicates transitions with no firm coincidence relations. The energy uncertainties are within the intrinsic resolution of the RISING array.

Precursor	E_x(keV)	E_γ(keV)	I_γ (%)	Coincident γ rays
^{211}Tl^{gs}	438	438	67(17)	316, 1395
88^{+46}_{-29} s	583	583	21(8)	
	597	597	100(24)	362, 1190
	754	316	73(18)	438, 1395
	1787	1190	102(27)	362, 597
	2149	362	74(18)	597, 1190
		1395	5(5)	754, 438
^{212}Tl^{gs}	804	804	100(23)	157, 315
96^{+42}_{-38} s	1119	315	79(18)	804
	1276	157*	11(4)	
^{213}Tl^{gs}	675	675	100(29)	
46^{+55}_{-26} s				
^{215}Pb^{gs}	185	185	100(47)	
160(40) s				
^{215}Bi^{gs}	271	271	6.8(1.0)	805, 1022
456(12) s	293	293	100(8)	785
	402	402	1.4(5)	
	517	517	4.7(9)	776
	835	564	1.5(5)	
		835	1.5(6)	
	877	877	1.3(5)	
	1009	1009	0.9(5)	
	1076	785	0.6(4)	293
		805	0.8(4)	271
		1075	2.7(8)	
	1150	1150	1.8(7)	
	1293	776	2.0(7)	517
		1022	0.7(4)	271
	1398	1105	2.2(8)	
		1399	0.3(3)	
^{215}Bi^{m}	293	293*	100(12)	226, 256, 308, 419, 498
36.9(6) s	712	419	80(12)	226, 256, 293, 308
	1020	308	90(14)	141, 226, 256, 498
	1246	226	90(12)	256, 293, 308, 419
	1502	256	84(10)	KX Po, 141, 226
				293, 308, 419, 498
	1643	141*	19(13)	154, 226, 256, 308, 419
	1999	498	58(5)	256, 293, 308, 419
		154†		141, 226, 256, 308, 419
^{216}Bi^{gs}	549	549	100(7)	KX Po, 187, 223, 251, 283
133(15) s				322, 359, 418, 485, 534
				580, 682, 758, 1461
	967	418	71(5)	KX Po, 187, 223, 251, 359
				534, 549, 580, 740, 758
	1326	359	55(4)	KX Po, 223, 251, 304,
				322, 418, 488, 549, 682
	1549	223	34(3)	KX Po, 158, 251, 322
				359, 418, 485, 549, 682
	1696	147	3.4(5)	KX Po, 223, 251
				359, 418, 549
	1800	251	7.6(9)	147, 223, 359, 418, 549
	1871	322	2.3(5)	223, 359, 418, 549
	1977	428	0.6(3)	223, 251, 359, 418, 549
	2034	485*	4.5(8)	223, 359, 418, 549
	2231	682	4.7(8)	223, 359, 418, 549
^{216}Bi^{m}	1502	534	0.6(3)	225, 418, 549
		953	2.6(7)	549
	1547	580	8(1)	418, 549
	1708	740	1.3(4)	418
		1159	2.4(7)	549
	1725	758	6(1)	418, 549
	2010	1461	0.9(4)	349, 549
	2359	349	1.7(4)	198, 223, 549, 1461
^{217}Bi^{gs}	254	254	29(4)	446, 841
93(11) s	264	264	100(11)	160, 623, 889
	376	376	16(3)	
	554	554	17(3)	
	632	632	10(3)	
	700	446	3(1)	254
	757	757	16(4)	739
	887	623*	4(2)	264
	1095	841	4(2)	254
	1153	889	7(2)	160, 264
	1313	160*	1.7(8)	264, 889
	1496	739		757
^{218}Bi^{gs}	509	509*	120(11)	262, 385, 425, 537, 703
33(6) s	934	425	109(10)	262, 385, 509, 537, 703
	1319	385	100(9)	262, 425, 509, 537, 703
	1581	262*	48(5)	385, 425, 509, 703
	1856	537	9(2)	385, 509, 425
	2284	703	9(2)	262, 385, 509, 425

also predicts the existence of several positive-parity states within the Q_β window for this decay ($Q_\beta = 4410$ keV [35]). Therefore, the $(1/2^+)$ ground state of ^{211}Tl can decay to $3/2^+$ or $1/2^+$ levels in ^{211}Pb through allowed Gamow-Teller β transitions. The non-negligible β feeding of the 754-keV

TABLE II. γ-ray energies E_γ, relative γ intensities (normalized to the most intense γ peak) I_γ, and coincidence relations of the γ rays observed following β decay of the ground state of ^{219}Bi. The energy uncertainties are within the intrinsic resolution of the RISING array.

Precursor	E_γ (keV)	I_γ (%)	Coincident γ rays
	72	39(13)	
	163	14(6)	
	183	54(16)	264, 389, 564
	231	50(16)	
	264	45(15)	183
^{219}Bi$^{g.s}$	287	23(10)	
22(7) s	347	38(13)	374
	373	23(10)	348, 389, 564
	390	50(17)	182, 348, 375
	445	28(12)	
	462	14(8)	565
	564	100(29)	183, 373, 462

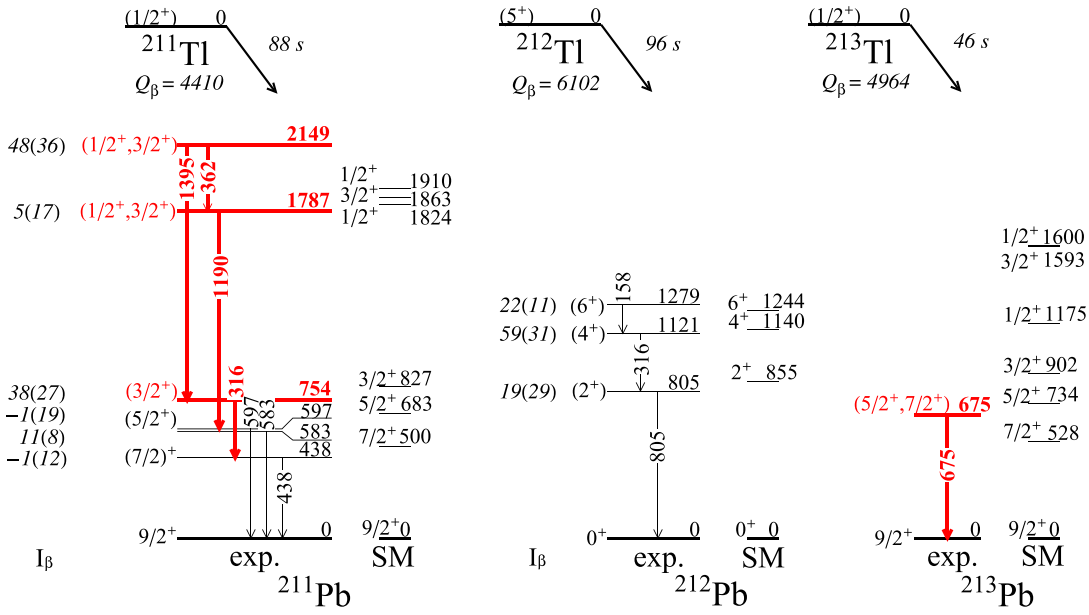

FIG. 9. (Color online) Experimental (exp.) and calculated (SM) partial level schemes of the $Z = 82$ isotopes $^{211–213}$Pb. New states and γ rays are indicated in bold red (gray) fonts. Half-lives and Q_β values, given in keV, are taken from Refs. [8,35]. β feedings (%) are obtained assuming $E2$ multipolarities for all transitions except the 362-, 438-, 1190-, and 1395-keV γ rays, for which an $M1$ character has been considered. See text for details.

level (see Fig. 9), which connects the $(1/2^+)$ ^{211}Tl ground state with the reported $(7/2)^+$ state at 438 keV, suggests a $J^\pi = (3/2^+)$ assignment. This is in good agreement with the location of the first $3/2^+$ state at 827 keV by shell-model calculations. Moreover, such a level was already predicted at 762 keV by Liang *et al.* [20], who inferred its energy from α-γ coincidences with the 438-keV transition.

Following the β-decay selection rules, we have proposed spin parities $1/2^+$ or $3/2^+$ for the experimental 1787- and 2149-keV states. This is in agreement with the SM calculations, which predict two $1/2^+$ states and one $3/2^+$ level at energies close to the experimental values (see Fig. 9).

Note that the missing of any sizable β feeding for the 438- and 597-keV states is expected from the previous $(7/2)^+$ and $(5/2^+)$ spin-parity assignments, as implied by β-decay selection rules. Indeed, from this consistency condition one can estimate $E2$ and $M1$ multipolarities for the transitions connecting the $(3/2^+) \rightarrow (7/2)^+ \rightarrow 9/2^+$ cascade, 316 and 438 keV. This is not the case for the 583-keV level, which connects the $(1/2^+)$ ground state in ^{211}Tl with the $9/2^+$ ground state in ^{211}Pb. The observed intensity is interpreted as a consequence of the pandemonium effect [40]: It must arise from fragmented γ feeding from higher lying states, with intensities undetectable by the current experimental setup.

Shell model calculations are in good agreement with the proposed β-decay scheme, exceeding the experimental values typically by less than 100 keV.

Figure 9 also shows the partial β-decay level scheme of ^{212}Pb, together with the shell-model calculations. The ground-state spin parity of the mother ^{212}Tl is expected to be 5^+ from systematics of neighboring nuclei [35]. This assumption is in agreement with our observations: The γ-ray spectrum of Fig. 6 shows evidence for the population of the (4^+) state through the 315 → 804 keV γ cascade. Further γ-γ coincidences with these two lines reveal some feeding to the higher lying (6^+) level [26], indicating that the main β transitions are of allowed Gamow-Teller type.

The first spectroscopic information available on ^{213}Pb is given in the γ spectrum of Fig. 6. A unique γ line at 675 keV is visible. Since it is not in coincidence with other transitions, it is likely to be a decay to the ground state or a decay which feeds into a long-lived isomeric state.

The mother ^{213}Tl is expected to have a $1/2^+$ ground state from systematics [35], and shell-model calculations support these predictions. In such a case, allowed Gamow-Teller β transitions are expected to populate $3/2^+$ or $1/2^+$ states in ^{213}Pb, in analogy with the ^{211}Tl → ^{211}Pb β decay. Direct feeding to the proposed $(9/2^+)$ ground state [41] is not expected as a consequence of the large spin difference.

The right part of Fig. 9 shows the tentative location of the 675-keV γ ray in the level scheme. Since the SM calculations predict the first $1/2^+$ and $3/2^+$ states far above the energy of the observed transition, and the sequential decay via the $5/2^+$ state is not expected to be isomeric, the intensity measured is interpreted as arising from fragmented and hence unobserved γ feeding from higher lying $1/2^+,3/2^+$ states. In this case, the spin parity of this level will most likely be $5/2^+$ or $7/2^+$.

B. Decay ^{215}Pb → ^{215}Bi

The β decay of ^{215}Pb proceeds more likely via a high-energy $(\nu g_{9/2},\pi h_{9/2})$ first-forbidden transition to the ground

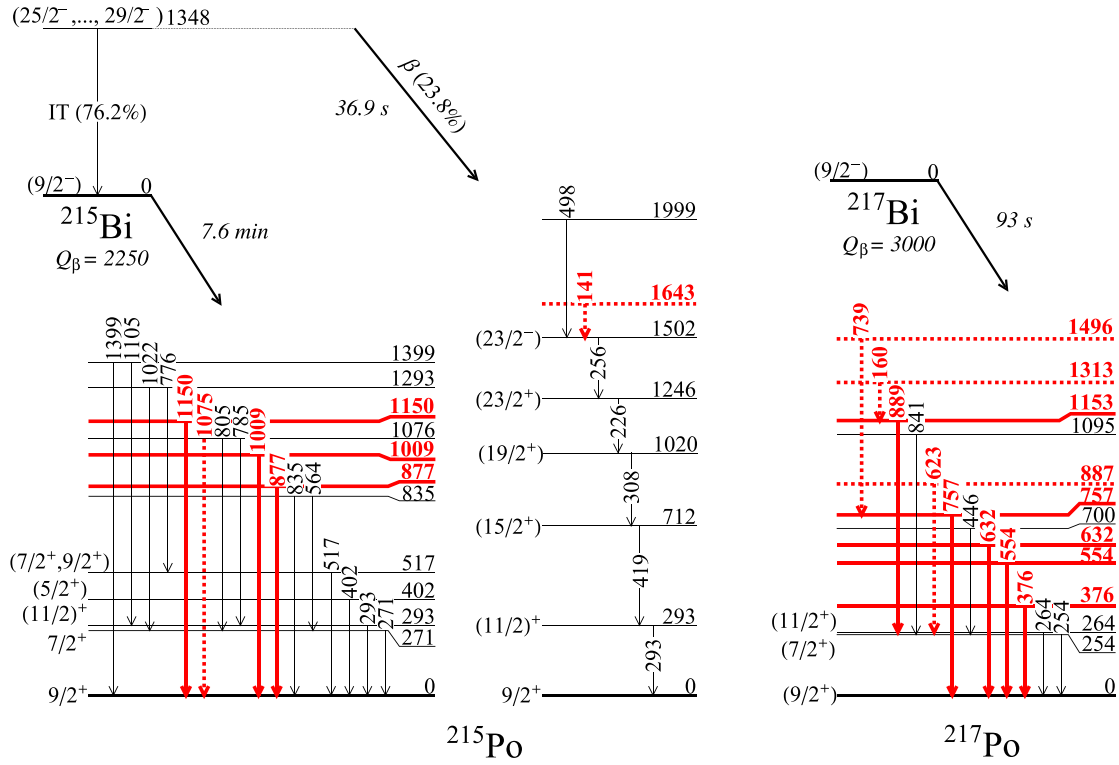

FIG. 10. (Color online) Experimental partial level schemes of the $Z = 84$ odd-A isotopes ^{215,217}Po. New states and γ rays are indicated in bold red (gray) fonts. Half-lives and Q_β values, given in keV, are taken from Refs. [8,35]. The decay branching ratios indicated for the high-spin isomer are taken from Ref. [13]. See text for details.

state of ^{215}Bi, as stated by recent β-decay studies of this nucleus carried out at CERN [10]. The γ-ray spectrum of ^{215}Pb, shown in Fig. 6, confirms the population of the first $(7/2^-)$ state in the daughter ^{215}Bi, also through a tentative high-energy first-forbidden transition. No coincident γ rays were found in this work, consistent with the

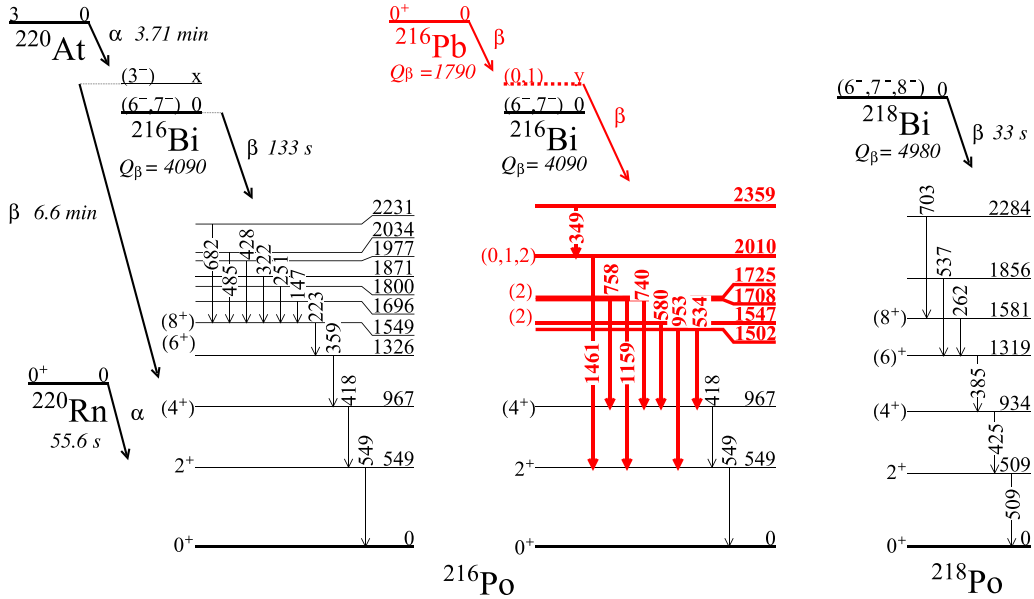

FIG. 11. (Color online) Experimental partial level schemes of the $Z = 84$ even-A isotopes ^{216,218}Po. New states and γ rays are indicated in bold red (gray) fonts. Half-lives and Q_β values are taken from Refs. [8,35]. See text for details.

available statistics and the apparent β feedings reported in Ref. [10].

C. Decays $^{215-219}$Bi → $^{215-219}$Po

The population of new levels in ^{215}Po is quite unexpected since the progenitors ^{215}Pb, ^{219}Bi, and ^{219}Po, implanted in the active stopper, decay via the ground state of ^{215}Bi. The observation of transitions differing from those reported in the β-decay studies of Kurpeta *et al.* [13] might be due to the more severe background in the previous work due to the diffusion of long-lived Rn isotopes through the separator. The new γ peaks at 877, 1009, 1075, and 1150 keV are visible in the α-tagged γ spectrum of Fig. 7. They are tentatively placed as ground-state transitions in Fig. 10 since they do not show any coincidence with other γ lines. The remaining γ peaks were reported in the former β decay work as well [13].

The γ ray at 877 keV was already observed in ^{219}Rn α-decay spectroscopy, de-exciting a state of the same energy with a hindrance factor (HF) of 2500 [2]. The 1075-keV γ ray can be interpreted as the ground-state decay of either a 1076-keV level reported in the previous β-decay work [13] or a 1073.7-keV state observed following α decay of ^{219}Rn [2]. In the first case, the direct transition to the ground state was not observed, whereas in the second the low HF of 32 for the 1073.7-keV decay suggested a $J^\pi = (5/2^+)$ assignment, in conflict with a direct β decay from the $(9/2^-)$ ground state of ^{215}Bi. In the level scheme shown in Fig. 10, it has been assigned as the direct ground-state de-excitation of the 1076-keV level, though, for the reasons described above, its placement is tentative. Note that if the location proposed here is the real one, possible spin parities for this state would be $J^\pi = (7/2^+, 9/2^+, 11/2^+)$.

Additionally, a newly observed γ ray at 141 keV shows mutual coincidence with the γ-ray cascade 226 → 308 → 419 → 293 keV arising from the high-spin β-decaying isomer. This transition is not seen above the background in the γ singles nor in the work by Kurpeta *et al.* [13]. Due to the low statistics, it is not possible to state whether it is also in coincidence with the 256-keV γ line or not, so its location in the level scheme is also tentative. The γ spectrum of ^{216}Po (see Fig. 7) shows 11 new γ-ray transitions, 8 of which can be tentatively located in the level scheme presented in Fig. 11. The placements are based on the relative intensities and coincidence relations listed in Table I.

Since these γ peaks were not reported in the β-decay work of ^{216}Bi by Kurpeta *et al.* [12], the new low-lying structure can be interpreted as arising from the β decay of the 0^+ ground state of ^{216}Pb. This, following the β-decay selection rules for the nuclei in this region [37], must feed $J^\pi = (0,1)^\pm$ states in ^{216}Bi. The internal de-excitation must populate a β-decaying isomer, giving rise to the new partial structure. This possibility is supported by the energy splitting of the 0^- to 9^- multiplet given by the parabolic rule of Paar [42], shown in Ref. [12], where the energy difference between the members of the multiplet is expected to be less than 300 keV. Spins of $2\hbar$ have been proposed for the states decaying to the reported (4^+) level, whereas tentative (0,1,2) assignments are suggested for the other states.

It is worth mentioning that no lifetime measurement has been performed for the newly proposed long-lived state in ^{216}Bi since the scarce statistics and the unknown β decay half-life of ^{216}Pb hinder a statistically significant measurement from the present data.

Figure 11 shows the known partial level scheme of ^{216}Po, previously reported in Ref. [12]. The relative intensities, listed in Table I, vary significantly from the former experiment. These discrepancies might be due to the simultaneous production of ^{216}Pb, ^{216}Bi, and ^{220}Po, whose decay chains feed the α emitter ^{216}Po (see Fig. 4).

The previous β-decay studies of ^{216}Bi [12] report the γ-ray cascade 223 → 359 → 418 → 549 keV, interpreted as de-exciting an 8^+ state by stretched $E2$ transitions. As pointed out in Ref. [12], the most probable spin parity for the ground state of ^{216}Bi is 6^- or 7^-, which is consistent with the strong population of the 6^+ level in ^{216}Po through a high-energy first-forbidden β transition.

Shell-model calculations performed *ad hoc* for this nucleus predict a degeneracy of the 3^-, 6^-, and 7^- ground-state candidates, being the energy splitting below 30 keV. Such degeneracy would explain the discrepancies with the ^{220}At α-decay data [43]: In this case, the (3−) ground-state candidate of ^{216}Bi is fed from the $J = 3$ ground state of ^{220}At, as indicated by the low HF of 3.2 of the α transition [35]. Thus, the β decay to ^{216}Po feeds mainly the (4^+) state. However, when ^{216}Bi is produced in spallation or fragmentation reactions, the (6^-) and (7^-) ground-state candidates are also populated, and the β-decay pattern to ^{216}Po is extended, as shown in the left part of Fig. 11.

In the γ spectrum of ^{217}Po (see Fig. 7) four new transitions emerge from the background at energies of 376, 554, 632, and 757 keV. The first three peaks do not show any coincidence with other γ lines, whereas the peak at 757 keV is in coincidence with the γ transition at 739 keV, as Fig. 8 shows. The ordering of the cascade has been chosen according to the relative intensities listed in Table II. The extended level scheme is shown in Fig. 10, where eight new excited states are suggested.

As for ^{215}Po, the population of new levels is not expected in ^{217}Po, since ^{217}Pb is expected to decay directly to the ground state of the daughter through a first-forbidden β transition [shell model predicts spin parities $(9/2^+)$ and $(9/2^-)$, respectively]. Moreover the accumulated statistics for ^{217}Pb only represent 8% of the implantations of ^{217}Bi.

From the γ-γ coincidence spectra of Fig. 8 some discrepancies with the previous β-decay work [14] appear: There is no hint of the 436- and 1017-keV transitions, whereas new γ peaks at 160 and 623 keV show coincidence with the 264-keV transition. In Ref. [14], the 889-keV γ line was identified in coincidence with the 254- and 264-keV transitions and was placed on top of the 436 → 264 keV cascade. Here it is seen in coincidence with the reported 264-keV γ ray and the new 160-keV transition, giving rise to the proposed 160 → 889 → 264 keV cascade.

In Ref. [22] the spin parity of ^{217}Po was suggested to be $11/2^+$. This assumption was derived from the small α-decay HF of 16 measured for ^{221}Rn, which indicated that the $7/2^+$ ground state, associated to the $1i_{11/2}$ shell-model state, had a configuration similar to the ground state of ^{217}Po. However, subsequent α-decay studies performed by the same authors [41] found an α-decay HF of 1.3 for ^{217}Po, implying no

change in configuration in going from the ground state of ^{217}Po to the ground state of ^{213}Pb, and suggesting, as well, the existence of an unobserved $9/2^+$ ground state lying just below the $11/2^+$ state in ^{217}Po. However, if there is a ground state in ^{217}Po lying just below the level populated by the 254- and 264-keV γ rays, one expects to observe, at least, a $M1$ or $E2$ transition with slightly higher energy connecting the two states. The absence of such a transition in both α- and β-decay studies, as well as the similarities between the partial β-decay level schemes of ^{215}Bi and ^{217}Bi (see Fig. 10), have led us to support the spin parities proposed in Ref. [14].

At variance with the $N = 132$ isotope, no β-decaying high-spin trap is observed, in agreement with the parallel isomer studies of the present data set [44]. These indicate that the analogous $J^\pi > 23/2^-$ isomer in ^{217}Bi de-excites 100% internally with a half-life of 2.70(6) μs.

The β decay of ^{218}Bi was already reported in Ref. [9]. No additional spectroscopic information has been obtained from the present data, since ^{218}Po is mainly produced from the β-precursor residue ^{218}Bi. The partial β-decay level scheme is shown in Fig. 11. The γ-ray ordering and apparent β feedings of Ref. [9] are nearly reproduced, except for some low-intensity transitions that are not observed in the current work. Also the half-life measured with this data set, $t_{1/2} =$ 33(6) s [8], is in agreement with the previous result.

Looking at Fig. 11, the β-decay pattern of ^{218}Bi is very similar to that of the $(6^-,7^-)$ ground-state decay of ^{216}Bi. This feature, together with the strong β feeding of the (6^+) 1319- and (8^+) 1581-keV states, suggests a $J^\pi = 6^-$, 7^-, or 8^- assignment for the ground state of ^{218}Bi, built from the $(\pi 1h_{9/2})(\nu 2g_{9/2})$ multiplet. The β decay must transform a neutron in the $2g_{9/2}$ orbital into a proton in the $1h_{9/2}$ subshell through a high-energy first-forbidden β transition, in accordance with the interpretation proposed in Ref. [9].

From the γ spectrum of Fig. 6, twelve γ transitions have been identified in the β decay ^{219}Bi $\rightarrow$ ^{219}Po. The low statistics and the complicated coincidence relations (see Table II) prevent from building any level scheme. However, from systematics, the mother ^{219}Bi is expected to have a $(9/2^-)$ ground state arising from the unpaired proton in the $1h_{9/2}$ shell. Accordingly, one would expect the $(\pi 1g_{9/2},\nu 1h_{9/2})$ single-particle β configuration to drive first-forbidden transitions to β-decay daughter states built, mainly, on the $(\pi 1h_{9/2})^{(2)}$ component.

D. β-decay systematics beyond ^{208}Pb

The feeding pattern of ^{212}Pb may suggest, despite the large uncertainties, an allowed Gamow-Teller nature for the decay of the mother ^{212}Tl. From a theoretical viewpoint, this feature can be understood in terms of the microscopic structures of mother and daughter nuclei: Direct single-particle β decays are completely blocked because the ground states of the $N > 126$ Tl isotopes have a proton hole in the $s_{1/2}$ orbital, while the valence neutrons lie within the $g_{9/2}$ and $i_{11/2}$ subshells. The large spin differences imply that the β transitions must be driven by the Gamow-Teller $(\nu i_{11/2},\pi i_{13/2})$ or first-forbidden $(\nu g_{9/2},\pi h_{9/2})$ single-particle components. In order to clarify which configuration is favored, we performed SM calculations allowing one proton excitation from the ^{208}Pb core. Two main features have been drawn: First, the occupation number of the $i_{11/2}$ neutron subshell is nearly one for the Tl ground states, and, second, the calculations indicate that the $\pi i_{13/2}$ single-particle orbital is fragmented over several low-lying states in the Pb daughters due to correlations between nucleons, with an increasing presence for larger excitation energies. This would favor the existence of Gamow-Teller β transitions with increasing intensities for higher-lying states. The systematics of measured half-lives also support this interpretation: Calculated lifetimes using the FRDM+QRPA approach [3] underestimate the experimental values typically by a factor two, as shown in Fig. 4 of Ref. [8]. This model, based on the quasiparticle random-phase approximation (QRPA) on top of the microscopic-macroscopic finite-range droplet mass model (FRDM), confers a minor role to the first-forbidden strength and enhances β transitions of allowed Gamow-Teller character. Unfortunately, given the present data, no firm conclusion on the nature of the observed states can be drawn, thus further studies to confirm the role of the $(\nu i_{11/2},\pi i_{13/2})$ β configuration in these nuclei are needed.

At variance with the Tl isotopes, the presence of allowed transitions is not expected for the Pb and Bi nuclei discussed in this work. Instead, high-energy first-forbidden β-decay transitions are predicted to appear once the $Z = 82$ major shell is filled, mainly arising from the transformation of a neutron in the $2g_{9/2}$ orbital into a proton in the $1h_{9/2}$ shell. For these nuclei, self-consistent microscopic approaches, such as the new DF3+cQRPA [4], agree within a factor two with the experimental half-lives [8]. In contrast to the FRDM+QRPA theory, this model treats the β-decay strength of Gamow-Teller and first-forbidden character within a fully self-consistent microscopic framework. The microscopic-macroscopic model, instead, deviates up to a factor ten [8].

VII. CONCLUSIONS

The β decays of neutron-rich Tl, Pb, and Bi isotopes have been investigated following fragmentation of a relativistic ^{238}U beam. Tentative level schemes of $^{211–213}$Pb and $^{215–218}$Po have been built from γ singles and γ-γ coincidence spectra and, where possible, spins and parities have been suggested from a coherent assessment of systematics, shell-model predictions, and β-decay selection rules. The β-decay of ^{215}Pb has been also studied, confirming the half-life and the associated 185-keV γ ray in ^{215}Bi, recently measured at the isotope separator online (ISOLDE).

Results from this and other work on lifetimes suggest that allowed β transitions might be opened in $N > 126$ Tl isotopes, while for Pb and Bi neutron-rich nuclei self-consistent microscopic models expect a dominant role of first-forbidden transitions.

Since predictions of r-process time scales and β-decay rates require exhaustive knowledge on β-strength functions, these first experimental evidences call for future measurements in the neutron-rich region above $N = 126$.

Further experimental access will be possible in the next generation of secondary beam facilities, where the very intense primary beams and new technological developments will allow for detailed nuclear spectroscopy.

In the meanwhile, theoretical efforts aiming at describing comprehensively β-decay properties towards the neutron-drip line can be of great guidance. In this sense, nuclear models based on the same microscopic ground-state description represent a more reliable, self-consistent tool to be used in calculations of stellar nucleosynthesis.

ACKNOWLEDGMENTS

The authors acknowledge the support of the Italian INFN and the Spanish MICINN through the AIC10-D-000568 bilateral action; the MICINN and the Generalitat Valenciana, Spain, under Grants No. FPA2008-06419, No. FPA2012-24553, and No. PROMETEO/2010/101; the STFC and EPSRC (UK); the Swedish Research Council, the Hungarian OTKA under Contract No. T104543; and the DFG (EXC 153). The excellent work of GSI accelerator staff is also acknowledged.

[1] P. Butler and W. Nazarewicz, Rev. Mod. Phys. **68**, 349 (1996).
[2] C. F. Liang, P. Paris, and R. K. Sheline, Phys. Rev. C **59**, 648 (1999).
[3] P. Möller, B. Pfeiffer, and K.-L. Kratz, Phys. Rev. C **67**, 055802 (2003).
[4] I. N. Borzov, Phys. Rev. C **67**, 025802 (2003).
[5] T. Suzuki, T. Yoshida, T. Kajino, and T. Otsuka, Phys. Rev. C **85**, 015802 (2012).
[6] T. Kurtukián-Nieto *et al.*, Nucl. Phys. A **827**, 587 (2009).
[7] A. I. Morales *et al.*, Phys. Rev. C **88**, 014319 (2013).
[8] G. Benzoni *et al.*, Phys. Lett. B **715**, 293 (2012).
[9] H. De Witte *et al.*, Phys. Rev. C **69**, 044305 (2004).
[10] H. De Witte *et al.*, Phys. Rev. C **87**, 067303 (2013).
[11] R. Broda, J. Phys. G: Nucl. Part. Phys. **32**, R151 (2006).
[12] J. Kurpeta *et al.*, Eur. Phys. J. A **7**, 49 (2000).
[13] J. Kurpeta *et al.*, Eur. Phys. J. A **18**, 31 (2003).
[14] J. Kurpeta *et al.*, Eur. Phys. J. A **18**, 5 (2003).
[15] M. Pfützner *et al.*, Phys. Lett. **444**, 32 (1998).
[16] H. Álvarez-Pol *et al.*, Phys. Rev. C **82**, 041602 (2010).
[17] G. Lane *et al.*, Phys. Lett. B **606**, 34 (2005).
[18] C. Ellegaard *et al.*, Nucl. Phys. A **259**, 435 (1976).
[19] C. Ellegaard *et al.*, Nucl. Phys. A **170**, 209 (1971).
[20] C. F. Liang, P. Paris, and R. K. Sheline, Phys. Rev. C **58**, 3223 (1998).
[21] W. Kurcewicz *et al.*, Nucl. Phys. A **289**, 1 (1977).
[22] C. F. Liang, P. Paris, and R. K. Sheline, Phys. Rev. C **56**, 2324 (1997).
[23] K. Hyde and A. Ghiorso, Phys. Rev. **90**, 267 (1953).
[24] L. Madansky and F. Rasetti, Phys. Rev. **102**, 464 (1956).
[25] E. Ruchowska *et al.*, J. Phys. G: Nucl. Part. Phys. **16**, 255 (1990).
[26] A. Gottardo *et al.*, Phys. Rev. Lett. **109**, 162502 (2012).
[27] A. Gottardo *et al.*, Phys. Lett. B **725**, 292 (2013).
[28] K.-H. Schmidt *et al.*, Nucl. Instrum. Methods A **260**, 287 (1987).
[29] A. I. Morales *et al.*, Phys. Rev. C **84**, 011601 (2011).
[30] S. Pietri *et al.*, Nucl. Instrum. Methods B **261**, 179 (2007).
[31] R. Kumar *et al.*, Nucl. Instrum. Methods A **598**, 754 (2009).
[32] N. Alkhomashi *et al.*, Phys. Rev. C **80**, 064308 (2009).
[33] N. Al-Dahan *et al.*, Phys. Rev. C **85**, 034301 (2012).
[34] G. Benzoni *et al.*, EPJ Web of Conferences (to be published).
[35] ENSDF, http://www.nndc.bnl.gov/ensdf/.
[36] H. Bateman, Proc. Cambridge Philos. Soc. **15**, 423 (1910).
[37] I. Borzov, Phys. Atom. Nucl. **74**, 1435 (2011).
[38] E. Caurier and F. Nowacki, Act. Phys. Pol. B **30**, 705 (1999).
[39] E. K. Warburton and B. A. Brown, Phys. Rev. C **43**, 602 (1991).
[40] J. Hardy *et al.*, Phys. Lett. B **71**, 307 (1977).
[41] C. Liang *et al.*, Czec. J. Phys. **54**, 189 (2004).
[42] V. Paar, Nucl. Phys. A **331**, 16 (1979).
[43] D. Burke *et al.*, Z. Phys. A **333**, 131 (1989).
[44] A. Gottardo, Ph.D. thesis, Università degli Studi di Padova, 2012 (unpublished).